JP1.14 MICROPHYSICAL INTERPRETATION OF CIRRUS MEASUREMENTS WITH LIDAR - COMPARISON TO A COUPLED OPTICAL-MICROPHYSICAL MODEL

Jens Reichardt[1,2,*], Ruei-Fong Lin[3,4], Susanne Reichardt[1,2], Thomas J. McGee[2], David O'C. Starr[4]

[1]Joint Center for Earth Systems Technology, University of Maryland Baltimore County, Baltimore, Maryland
[2]Laboratory for Atmospheres, Code 916, NASA Goddard Space Flight Center, Greenbelt, Maryland
[3]Goddard Earth Sciences and Technology Center, University of Maryland Baltimore County, Baltimore, Maryland
[4]Laboratory for Atmospheres, Code 912, NASA Goddard Space Flight Center, Greenbelt, Maryland

1. INTRODUCTION

Recently, Reichardt et al. (2002a) reported lidar measurements of Arctic and northern mid-latitude cirrus clouds which showed that (1) the particle optical properties, specifically depolarization ratio δ_{par} and extinction-to-backscatter ratio S, were strongly correlated, (2) over the length of each cirrus measurement, the particle properties varied systematically, and (3) the particle optical properties distinctly depended on the ambient temperature. Based on ray-tracing computations of particle scattering properties, Reichardt et al. (2002b) interpreted these measurements in terms of size, shape and growth of the cirrus particles. According to the interpretation of Reichardt et al. (2002b), light scattering by small hexagonal columns with aspect ratios close to one was dominant near the cloud top in the early stage of the cirrus development. Over time, as the cloud base extended to lower altitudes with warmer temperatures, the ice particles grew larger and became morphologically diverse: the optical lidar signature was indicative of a mixture of column- and plate-like particles (particles that have the scattering properties of hexagonal columns or plates, respectively). Toward the cloud base, light scattering was predominantly by plate-like ice particles.

Since no *in situ* data of particle microphysical properties are available for comparison, we test the proposed explanation of the lidar data for consistency with a coupled microphysical and optical cirrus model. We look at the development of cirrus clouds over time. For a first case study, the cirrus measurement taken on 16 January 1997 above the Esrange (67.9°N) research facility in northern Sweden was selected, which clearly shows all previously summarized characteristics of the cirrus observations (Fig. 1). In Section 2, a brief description of the coupled optical-microphysical model is given. In Section 3, synthetic and measured optical properties are compared.

2. COUPLED OPTICAL-MICROPHYSICAL MODEL

A modified version (see Section 2.1) of the microphyiscal cirrus model of Lin (1997) is employed for generation of the cloud microphysical properties for measurement segments A and B (Fig. 1). Temperatures are taken from a radiosonde measurement at Luleå ($\sim$200 km south of the lidar site) during the lidar observation. The vertical wind speed is assumed to be height- and time-independent. This

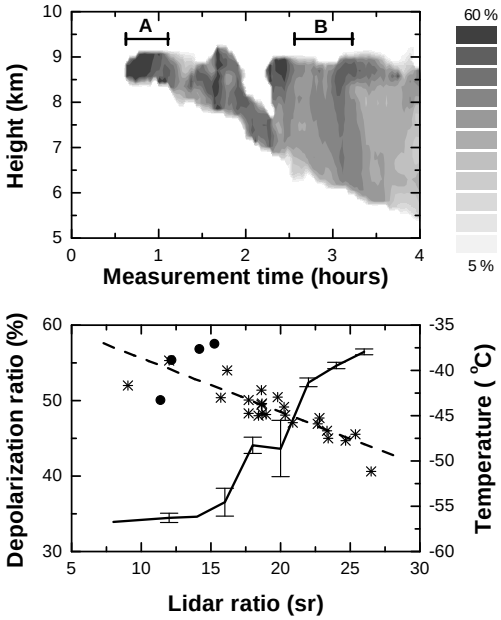

Figure 1: Height versus time display of particle depolarization ratio generated from consecutive lidar profiles of the cirrus cloud measured on 16 January 1997 over northern Sweden (top). The measurement wavelength is 355 nm. Particle depolarization ratio versus lidar ratio scatter plot of cirrus measurement segments A (●) and B (*) marked in the top panel (bottom). δ_{par} and S of the data set are strongly correlated (correlation coefficient of -0.82), the regression line is shown (dashed line). Cloud temperatures associated with the particle optical data are also shown (solid curve; averaged over 2-sr S bins). Error bars indicate statistical uncertainties of the temperature means. Temperature profiles are taken from a simultaneous radiosonde ascent at a near-by radiosonde station.

parameter and the humidity profile are deduced from sensitivity tests where the values selected yield the best agreement between (1) the observed and modeled cirrus geometrical properties (cloud height and vertical extent), and (2) the contours of the observed particle extinction profile and the modeled ice mixing ratio profile for both segments, and for which the simulation time span between model profiles A and B is about the same as the time interval between the measurement segments A and B.

Sensitivity tests with regard to the assumed particle shape show that generally results obtained for hexagonal columns or plates do not differ significantly in both integrated and mass-resolved parameters (as demonstrated by the intercomparison presented in Fig. 2). For this reason, we perform our cirrus simulations under the assumption

* *Corresponding author address:* Jens Reichardt, Laboratory for Atmospheres, Code 916, NASA Goddard Space Flight Center, Greenbelt, MD 20771; email: reichardt@code916.gsfc.nasa.gov

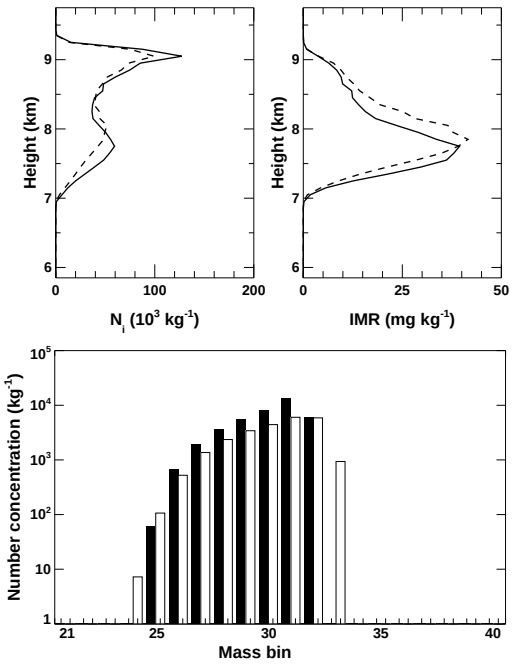

Figure 2: Integrated particle number concentration (top, left) and ice mixing ratio (top, right) for model runs with exclusively hexagonal columns (solid curves), or plates (dashed curves). The simulation time is 120 min. Mass-resolved particle number concentration for columns (solid bars) and plates (open bars) at a height of 7.45 km.

of columnar particle habit, and consider the microphysical model results as representative for hexagons of all aspect ratios.

The simulated mass-resolved data are then converted to cloud optical properties by use of optical data obtained with a ray-tracing model (Hess et at. 1998). Dependence of particle habit on particle nucleation temperature, and relations between aspect ratio and maximum dimension of the planar and columnar crystals can be varied to study the effect of cirrus particle populations with same particle size distribution (parameterized in terms of particle mass) but different morphologies on the optical properties. The parameters of the optical model are detailed in Section 2.2.

2.1 Microphysical Model

The cirrus model used in this study is a one-dimensional (spatial) model in which size distributions of ice crystals are explicitly resolved and their evolution due to diffusional growth, aggregation, and differential sedimentation is explicitly simulated (Lin 1997). In order to account for a nucleation temperature-dependent crystal habit in our optical simulation, the model has been modified to keep track of the nucleation temperatures of the ice particles. Model output now includes the nucleation temperature distribution of the cirrus particles for each mass bin at each height grid box. For the simulations presented here, the height resolution is 100 m, and the time increment is 0.1 s. Nucleation temperature is resolved in 1-degree intervals between -73 and -33°C. Particle mass spectra are registered

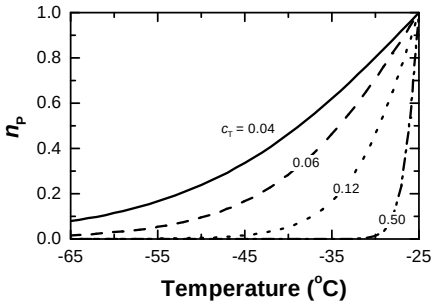

Figure 3: Mass fraction of plate-like cirrus particles as a function of nucleation temperature for values of model parameter c_T.

in 50 mass bins between 3×10^{-15} and 2×10^{-5} kg, the bin width increases exponentially. Mass bins 5, 15, 25, and 35 correspond with particle maximum dimensions of 4, 17, 67, and 520 μm, respectively [Column aspect ratios according to Auer and Veal (1970)]. The parameterization scheme of Meyers et al. (1992) for deposition nucleation is adopted. For the simulations performed for this weak lifting, heterogeneous nucleation is the dominant nucleation mode, homogeneous nucleation of aqueous solution droplets does not become active.

2.2 Optical Model

According to laboratory experiments, ice crystals growing at temperatures $<$-25°C should be principally of columnar shape (Mason et al. 1963). However, *in situ* particle sampling in cirrus clouds at these cold temperatures show particles of diverse morphology, including irregular and planar particles, and aggregates (see, e. g., Heymsfield and Iaquinta 2000). In order to account for particles with different habits in our model, we assume that two optically distinct classes of atmospheric particles exist, and that the fractional contribution of these particle groups to the lidar signature depend on the particle nucleation temperature. Since the theoretical optical data obtained for solid hexagonal columns and plates mark the upper and lower boundary, respectively, of our polarization Raman lidar measurements of cirrus clouds (Reichardt et al. 2002b), we identify column-like and plate-like particles as the two classes of scatterers. Mass fraction of plate-like cirrus particles n_P, and hence of the column-like particles, is controlled by model parameter c_T. The functional dependence on nucleation temperature is chosen in such a way that at -25°C all nucleated particles develop a planar shape. Figure 3 illustrates the dependence of n_P on c_T and temperature.

Field studies show that in natural ice clouds aspect ratio and size of the cloud particles are correlated. Generally, aspect ratios of columnar and planar particles, respectively, increase and decrease with size, although the actual functional relations seem to depend strongly on the atmospheric conditions (Ono 1969; Auer and Veal 1970). To allow for variability in the aspect-ratio to size relationship of columns and plates, we have included the parameters b_C and b_P in our optical model. The effect of both parameters on the aspect ratios of columns and plates is shown in Fig. 4. Also shown in Fig. 4 are the theoretical optical properties used to

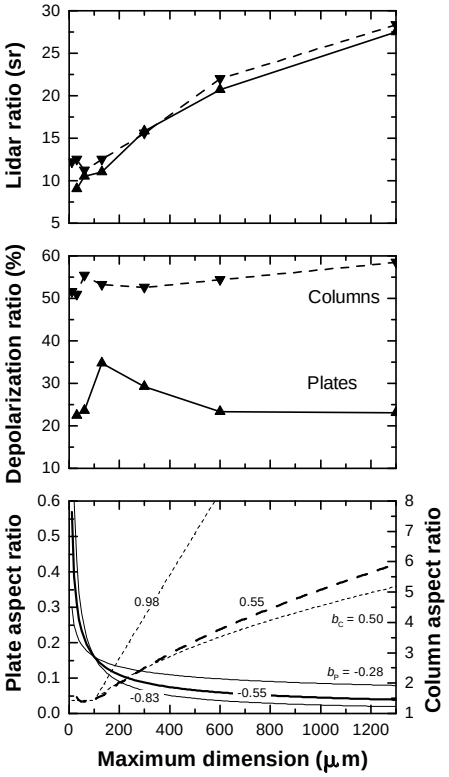

Figure 4: Lidar ratio (top), and depolarization ratio (center) versus ice-particle maximum dimension for solid hexagonal columns and plates. Particle length-to-width (aspect ratio) relations of Auer and Veal (1970) are assumed. Aspect ratio of hexagonal columns (dashed curves) and plates (solid curves) as a function of particle maximum dimension (bottom). For columns, relations are plotted for b_C values of 0.50 (Mitchell and Arnott 1994), 0.55 (Auer and Veal 1970), and 0.98 (Ono 1969). For plates, b_P values of -0.83, -0.55 (Auer and Veal 1970), and -0.28 are chosen for illustration.

convert the results of the microphyical model data to synthetic lidar profiles. The theoretical optical data have been derived in the geometrical-optics approximation, therefore they only depend on the aspect ratio, but not on the size of the cirrus particle. However, because the size and the aspect ratio are correlated, the calculated optical properties are indirectly a function of particle size. Figure 4 illustrates that S is a sensitive indicator of particle size, whereas δ_{par} varies more with particle habit.

3. RESULTS

The best agreement of the modeled geometrical properties with the observed cirrus cloud during measurement segments A and B is found if an updraft wind speed of 0.07 m s^{-1} is assumed. The optimum initial humidity profile, which is also deduced from sensitivity tests, is characterized by a moist layer between 6.5 and 8.8 km, with maximum relative humidity (120%, with respect to ice) close to its upper boundary, and relatively dry air below 6.5 km. This is in accordance with lidar measurements of water vapor in the boundary layer and lower free troposphere (obtained simultaneously with the cirrus observation; due to low absolute relative humidity, water vapor data at cirrus altitudes are not available), which reveal a sharp increase in relative humidity at $\sim$6 km.

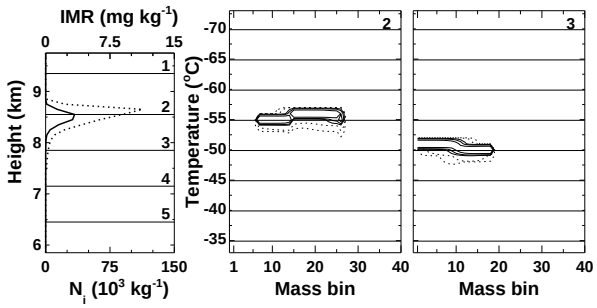

Figure 5: Modeled ice mixing ratio (solid curve) and particle number concentration (dotted curve) after 30 min of simulated time (left). Because modeled and observed cloud geometrical profiles are similar, the model at this time step is associated with the cirrus cloud as observed during measurement segment A. The other panels show nucleation temperature distribution (relative) as a function of particle mass for selected heights (height levels are marked in left plot). Outer and inner dashed, and outer, center, and inner solid contour lines indicate, respectively, 0.001, 0.01, 0.1, 0.2, and 0.4 levels.

Microphyiscal model results after 30 min of simulated cirrus evolution are presented in Fig. 5. The model cloud develops between 8 and 9 km, with maxima of ice mixing ratio and particle concentration around 8.6 km. At 8.55 km (height level 2), nucleation temperatures of the ice particles are predominantly between -54 and -57°C, particle sizes range between $\sim$5 and 75 μm. After 30 min, adiabatic cooling due to the imposed updraft has generated sufficient supersaturation at initially slightly ice-subsaturated height level 3 (7.85 km) to initiate particle nucleation (smallest crystals are in the size range of a few microns).

Because of the geometrical similarity with the cirrus observation around 1 hour measurement time (Fig. 1), the data shown in Fig. 5 is assumed to be representative of observation segment A. In order to find a model counterpart to measurement segment B, we modeled the evolution of the cirrus cloud for longer times, and compared measured and modeled geometrical profiles between 117 and 186 min of simulation time (which corresponds to the 87 to 156–min time span between observation periods A and B). Best agreement is found for a simulated time of 180 min (Fig. 6). The modeled cloud base and the maximum of the ice mixing ratio are at 6 and 6.7 km, respectively. Generally, from cloud top to bottom, nucleation temperatures shift to warmer temperatures, while the lower and upper boundaries of the particle spectra shift to larger particle masses (sizes). However, at height levels 4 and 5, a second mode of comparatively small particles with warmer nucleation temperatures (around -46°C) developed, that means a second generation layer was present at an altitude of 7.5 km. This might have indeed been the case on 16 January 1997, since the lidar data show elevated backscatter-coefficient values below this height.

The modeled optical properties are contrasted with the lidar observations for both measurement segments in Fig. 7.

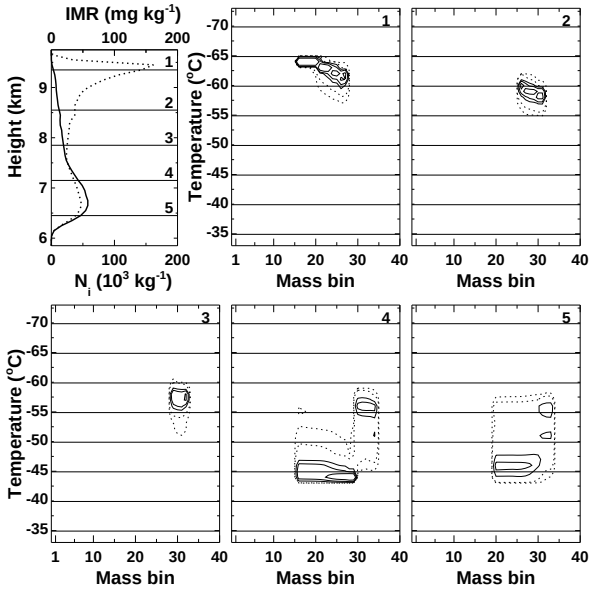

Figure 6: Same as in Fig. 5, but for measurement segment B (180 min simulation time).

The synthetic data shown have been selected from 30 optical model runs with different parameter sets (c_T, b_C, b_P). It turns out that these parameters can be chosen in such a way that modeled and observed data agree well.

The modeled extinction coefficient is insensitive to the model parameters, and maximum values are close to the largest extinction coefficients observed. Interestingly, the synthetic height profile of segment B, though shifted slightly to higher altitudes, has the same outline as the observation.

Measured depolarization ratios of segment B are fully reproduced by the coupled optical-microphyiscal model. For the same parameter set, however, modeled δ_{par} are 10% too low in measurement segment A. This is due to the contribution of plate-like particles to the cloud optical properties [at segment-A cloud center (-55°C), about 10% of the particles are planar, if $c_T = 0.05$]. If only columnar particles had been assumed ($c_T > \sim 0.1$), depolarization ratios of $\sim 55\%$ would have been modeled, but then δ_{par} would have been too high at lower cloud altitudes in segment B.

The lidar ratio, which is more sensitive to particle size than to crystal shape, is well simulated in both cases. Deviations from the observed S values near the segment-B cloud base are due to the height offset of the cloud profiles: below 6.7 km, model particles sublime and shrink in size, which results in decreasing lidar ratios (cf. data of height levels 4 and 5 in Fig. 6). The assumed b_C values (0.8–0.9) lie within the range of observations, they are closer to the data of Ono (1969) than to those collected by Auer and Veal (1970).

In summary, good agreement between lidar and synthetic data is found for all optical properties for the measurement periods considered. In view of the simplifying assumptions made about the dynamical forcing (time- and height-independent updraft wind speed), and the optical

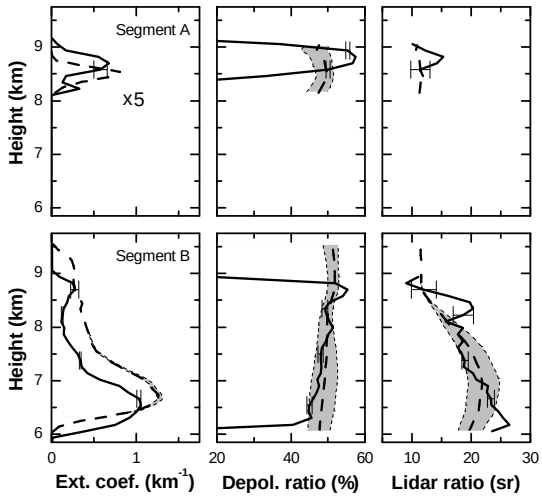

Figure 7: Observed (solid curves) and modeled [dashed curves; (c_T, b_C, b_P) = (0.05, 0.85, -0.55)] cirrus extinction coefficient, particle depolarization ratio δ_{par}, and lidar ratio S (from left to right) for the measurement segments marked in Fig. 1. Shaded areas indicate model results that are in reasonable agreement with the observations [parameter triplets for the left and right boundaries are (0.04, 0.80, -0.55) and (0.06, 0.90, -0.55), respectively]. Error bars indicate statistical noise of the measurements. Extinction coefficients of measurement segment A have been multiplied by a factor of 5.

model, observed differences are surprisingly small. These results support the proposed microphysical interpretation of cirrus measurements obtained with lidar (Reichardt et al. 2002b).

REFERENCES

Auer, A. H., Jr., and D. L. Veal, 1970: The dimension of ice crystals in natural clouds. *J. Atmos. Sci.*, **27**, 919–926.

Hess, M., R. B. A. Koelemeijer, and P. Stammes, 1998: Scattering matrices of imperfect hexagonal ice crystals. *J. Quant. Spectrosc. Radiat. Transfer*, **60**, 301–308.

Heymsfield, A. J., and J. Iaquinta, 2000: Cirrus crystal terminal velocities. *J. Atmos. Sci.*, **57**, 916–938.

Lin, R.-F., 1997: A numerical study of the evolution of nocturnal cirrus by a two-dimensional model with explicit microphysics. Ph. D. thesis (Pennsylvania State University, University Park), 199 pp.

Mason, B. J., G. W. Bryant, and A. P. van den Heuvel, 1963: The growth habits and surface structure of ice crystals. *Phil. Mag.*, **8**, 505–526.

Meyers, M. P., P. J. DeMott, and W. R. Cotton, 1992: New primary ice nucleation parameterizations in an explicit cloud model. *J. Appl. Meteorol.*, **31**, 708–721.

Mitchell, D. L., and W. P. Arnott, 1994: A model predicting the evolution of ice particle-size spectra and radiative properties of cirrus clouds. II. Dependence of absorption and extinction on ice crystal morphology. *J. Atmos. Sci.*, **51**, 817–832.

Ono, A., 1969: The shape and riming properties of ice crystals in natural clouds. *J. Atmos. Sci.*, **26**, 138–147.

Reichardt, J., S. Reichardt, A. Behrendt, and T. J. McGee, 2002a: Correlations among the optical properties of cirrus-cloud particles: Implications for spaceborne remote sensing. *Geophys. Res. Lett.*, revised.

——, ——, M. Hess, and T. J. McGee, 2002b: Correlations among the optical properties of cirrus-cloud particles: Microphysical interpretation. *J. Geophys. Res.*, submitted.